

# Effect of Ionic Liquids Pretreatment on the Extraction of Collagen from Calf Skin

by

Sicong Liu,<sup>1</sup> Wentao Liu,<sup>1\*</sup> and Guoying Li<sup>1,2\*</sup>

<sup>1</sup>National Engineering Laboratory for Clean Technology of Leather Manufacture, Sichuan University, Chengdu 610065, China

<sup>2</sup>Key Laboratory of Leather Chemistry and Engineering (Sichuan University), Ministry of Education, Chengdu 610065, China

## Abstract

The use of ionic liquids (ILs) for collagen extraction should be premised of not destroying the triple helix structure of collagen. Herein, the effects of pretreatments by two imidazolium based ILs with different anions, 1-ethyl-methylimidazolium dicyanamide ([EMIM][N(CN)<sub>2</sub>]) and 1-ethyl-methylimidazolium tetrafluoroborate ([EMIM][BF<sub>4</sub>]), on the extraction of collagen from calf skins were studied. The dependences of ILs pretreatments on ILs species and concentrations (30%, 50%, and 70% (w/w)) were examined, in terms of the fiber morphology of skins as well as the extraction rate, structural integrity, thermal stability, and aggregation behaviors of collagens. The results of histological analysis and scanning electron microscopy showed that the skin fibers were effectively loosened by the ILs pretreatments. The extraction rate of collagen was improved as the increase of ILs concentration and polarity with the highest value of 28.79%. Moreover, sodium dodecyl sulphate-polyacrylamide gel electrophoresis and Fourier transform infrared spectroscopy confirmed that the structural integrity of collagen was maintained after ILs pretreatments, although the thermal stability of collagen was determined to be slightly decreased by ultra-sensitive differential scanning calorimeter. Finally, pyrene fluorescence analysis and atomic force microscope indicated that the aggregation behavior of collagen was weakened when increasing the ILs concentration and polarity. The green ILs pretreatment of calf skins might be used as an effective approach for the extraction of bioactive collagen with improved yield and purity.

## Introduction

Collagen, a major structural protein of animal, is mainly distributed in connective tissues such as skin, tendon, and bone.<sup>1</sup> Its triple helix conformation contributed by two  $\alpha 1$  chains and one  $\alpha 2$  chain provides it with properties including exceptional biocompatibility, outstanding biodegradability, and weak

antigenicity.<sup>1-3</sup> As an important biomacromolecule, collagen has been widely applied in the fields of food, cosmetics, pharmaceuticals, and biomedicine.<sup>2-11</sup> Until now, collagen is mainly extracted from the connective tissues of land-based mammals (e.g. calf skin), which are common raw materials in leather industry. Such animal tissues are always tightly weaved and thereby are hard to be directly used to extract collagen. Generally speaking, some pretreatments prior to collagen extraction are necessary to loosen the fiber contexture of connective tissues and to remove non-collagenous impurities from the tissues,<sup>6-8</sup> just like the liming operation in leather manufacture.<sup>12-13</sup> Due to appropriate pretreatments, both the purity and extraction yield of collagen could be improved to a great extent.<sup>6-8</sup> However, any pretreatments should be on the premise of not destroying the triple helix structure of collagen.

Ionic liquids (ILs), composed of bulky organic cations and minor inorganic (or organic) anions, are classified as green solvents for their negligible vapor pressure, non-flammability, low toxicity, and outstanding solvation ability.<sup>9-30</sup> The physicochemical properties of ILs including viscosity, polarity, hydrophobicity, melting point, and hydrogen-bonding capability are highly dependent on the species of cations and anions.<sup>10,14</sup> Thus, the structure and properties of ILs can be finely and effectively tailored for a variety of applications (e.g., biotechnology and organic synthesis),<sup>22,28</sup> especially for the dissolution and extraction of biomacromolecules such as cellulose,<sup>29</sup> chitosan,<sup>30</sup> and collagen.<sup>9,10,15-20</sup> Although the influences of many different types of ILs on collagen have been extensively investigated,<sup>9-13,15-26</sup> little information is available concerning the use of ILs for the pretreatment of connective tissues before collagen extraction. Some investigations applied ILs to directly dissolve collagen fibers (white hide powder) at high temperatures (even  $\geq 100^\circ\text{C}$ ), whereas inevitably leading to the thermal denaturation and degradation of collagen.<sup>15-20</sup> Others first extracted acid-soluble collagen molecules and then explored the interactions between collagen and ILs, rather than focusing on the extraction of collagen.<sup>21-26</sup> Furthermore, it should be emphasized that both the

\*Corresponding author e-mails: scu.collagen@gmail.com (W. Liu); liguoyings@163.com (G. Li)

Manuscript received April 9, 2019, accepted for publication June 9, 2019

ion species and concentration of ILs have great impacts on the structural stability of collagen.<sup>11-14,20-26</sup> For instance, the differences in composition of imidazolium-based ILs endowed by varying anions namely dicyanamide, hydrogen sulfate, dimethyl phosphate, acetate, sulfate and dihydrogen phosphate, had brought about the different destabilizing effects on the triple helical structure of collagen;<sup>22</sup> a remarkable decreasing trend in denaturation temperature of rat tail tendon collagen fibers was observed with the increase of ILs concentration from 0.1% to 10% (w/v).<sup>11</sup> Therefore, it will be of importance and significance to study how the ILs pretreatments would affect the fiber contexture of connective tissues and the structure and properties of collagen, as well as to clarify how the extraction of collagen could be tuned by the ILs parameters.

In fact, two 1-butyl-3-methylimidazolium ([BMIM]) based ILs with different anions ( $[\text{BF}_4]^-$  and  $\text{Cl}^-$ ) have been verified to show excellent efficacies of fiber opening towards goat skins.<sup>11-13</sup> Mehta *et al.*<sup>11</sup> reported that the goat skin treated by 0.5% (g/g wt of skin) [BMIM]Cl displayed more pores with larger pore radii compared to the native skin. Jayakumar *et al.*<sup>13</sup> proposed the use of [BMIM]Cl as an eco-friendly approach to replace conventional liming in leather manufacture. Alla *et al.*<sup>12</sup> demonstrated that [BMIM] $[\text{BF}_4]$  could be used for an integrated depilation and fiber opening in leather processing. However, the current knowledge of ILs pretreatments for animal skins are limited to leather making. In contrast, we hypothesized that the use of ILs as a pretreatment agent to loosen collagen fibers in skins and to remove inter-fibrous non-collagenous components from the skin would be beneficial to the extraction of collagen. Herein, two types of 1-ethyl-3-methylimidazolium ([EMIM]) based ILs containing different anions, [EMIM] dicyanamide ([EMIM] $[\text{N}(\text{CN})_2]$ ) and [EMIM] tetrafluoroborate ([EMIM] $[\text{BF}_4]$ ), the ions of which exhibited good biocompatibility,<sup>9,12,27</sup> were used for the pretreatments of calf skins before collagen extraction. The effects of ILs pretreatments on fiber opening and morphology were studied by histological analysis and scanning electron microscope (SEM), and the extraction rate of collagen was compared under different conditions. The structural characteristics of calf skin collagen were examined by sodium dodecyl sulphate-polyacrylamide gel electrophoresis (SDS-PAGE) and Fourier transform infrared spectroscopy (FTIR), while the thermal stability of collagen was evaluated by ultra-sensitive differential scanning calorimeter (DSC). Moreover, the aggregation behavior of collagen was explored by fluorescence with a pyrene probe and atomic force microscope (AFM). The aim of this study was to give a greener pretreatment method to extract collagen with improved purity and yield.

## Experimental

### Materials

Calf skin was obtained from a local slaughterhouse in Chengdu, Sichuan province, China. First, the skin was unhaired and limed according to conventional leather processing operations, and then the limed skin was delimed and neutralized in a process described by Zhang *et al.*<sup>31</sup> The resultant dermis was cut into small pieces (5 mm × 5 mm) and referred to as natural skin (NS). The ionic liquids (ILs), 1-ethyl-3-methylimidazolium dicyanamide ([EMIM] $[\text{N}(\text{CN})_2]$ ,  $E_t(30) = 51.7$  kcal/mol) and 1-ethyl-3-methylimidazolium tetrafluoroborate ([EMIM] $[\text{BF}_4]$ ,  $E_t(30) = 53.7$  kcal/mol) were purchased from Lanzhou Institute of Chemical Physics (Chinese Academy of Sciences, Lanzhou, China) with high purification ( $\geq 99\%$ ). [EMIM] $[\text{N}(\text{CN})_2]$  and [EMIM] $[\text{BF}_4]$  were dissolved in deionized water at concentrations of 30%, 50%, and 70% (w/w), respectively. Pepsin was purchased from Sigma-Aldrich (MO, USA). All reagents used here were of analytical grade.

### Ionic Liquids Pretreatment on NS

The ILs ([EMIM] $[\text{N}(\text{CN})_2]$  and [EMIM] $[\text{BF}_4]$ ) at different concentrations were used to pretreat NS with the ILs/skin ratio of 10:1 (w/w) at 4°C with gentle stirring for 24 hours. Afterwards, the precipitate collected by refrigerated centrifugation (4°C, 9000g) was washed five times by distilled water. Moreover, ultrasound was used to further remove the residual ionic liquids for three times with a power of 50 W. All the ILs pretreated skins were named as IPS. Specifically, the skins pretreated by [EMIM] $[\text{N}(\text{CN})_2]$  at concentrations of 30%, 50%, and 70% (w/w) were referred to as APS30, APS50, and APS70, respectively, while those pretreated by [EMIM] $[\text{BF}_4]$  were correspondingly referred to as BPS30, BPS50, and BPS70, respectively.

### Histological Analysis

Histological analysis was performed to determine the dispersion extent of collagen fibers in IPS, according to the method of Li *et al.*<sup>6</sup> with some modifications. The IPS specimens were soaked in 10% (w/v) formalin solution for 24 h and then cut into 15- $\mu\text{m}$ -thick sections in transverse direction using a microtome (Jung Frigocut 2800 N, Leica Inc., Heidelberg, Germany). The specimens were stained with hematoxylin-eosin (H&E), followed by mounting in a neutral resin for observation with a light microscope (BH-2, Olympus, Tokyo, Japan).

### SEM

To investigate the effect of ILs pretreatment on the fiber structure of IPS, the morphology of IPS and NS were examined by a scanning electron microscope (ProX, Phenom, Netherlands) at an accelerating voltage of 15kV. Sequential treatments of the skin samples were performed according to Yunoki *et al.*<sup>32</sup> with slight modifications. Briefly, 2% (v/v) glutaraldehyde in 12 mM

phosphate buffered solution (PBS, pH~7.4) was used to immobilize skin samples for 30 min at 25°C. Then the samples were rinsed five times using deionized water, followed by successive dehydrating in a series of ethanol concentrations (30, 50, 70, 80, 90, 95, 99.5, and 100%, v/v). All samples were dried at 25°C before SEM measurements.

### Extraction of Collagen

Collagen was extracted from NS and IPS by the method of Zhang et al<sup>31</sup> with some modifications. First, the calf skins were dissolved in 0.5 M acetic acid containing 3% (w/w) pepsin with a sample/solution ratio of 1:40 (w/v) and collagens were extracted at 4°C for 48 h. Then the supernatants were collected by refrigerated centrifugation for 10 min at 9000g and 4°C, using a high speed refrigerated centrifuge (Kubota Corporation, Osaka, Japan). After centrifugation, NaCl was added into the supernatants to reach a final concentration of 0.7 M to salt-out collagen as precipitates. Subsequently, the precipitates were re-dissolved in 10 volumes of 0.5 M acetic acid. The resultant collagen solutions were continuously dialyzed against 20 volumes of 0.05 M acetic acid for three days with the change of dialyzing solution every half a day. The dialysates were lyophilized by a freeze-dryer (FreeZone 6 L, Labconco Co., Kansas, USA) at -50°C for three days and the freeze-dried collagens were stored in a desiccator. The collagen extracted from NS was referred to as natural collagen (NC), while that extracted from IPS was referred to as ILs pretreated collagen (IPC). Specifically, the collagen extracted from APS30, APS50, and APS70 were referred to as APC30, APC50, and APC70, respectively, while those extracted from BPS30, BPS50, and BPS70 were referred to as BPC30, BPC50, and BPC70, respectively.

### Extraction Rate of Collagen

The extraction rate (% w/w) of collagen was calculated on dry weight basis as following:

$$\text{Extraction rate (\%)} = (W_2 / W_1) \times 100 \quad (1)$$

where  $W_1$  is the dry weight of calf skin and  $W_2$  is the weight of the lyophilized collagen. All samples were measured in triplicate.

### SDS-PAGE

The electrophoretic patterns of collagens were determined by SDS-PAGE according to the method of Laemmli et al<sup>33</sup> with some modifications, involving a 7.5% resolving gel and a 4% stacking gel. Each collagen sample was mixed with 0.5 M Tris-HCl buffer (pH 6.8) solution containing 25% glycerol, 2% SDS, 10%  $\beta$ -mercaptoethanol, and 0.01% bromophenol blue to reach a final collagen concentration of 1 mg/mL. Then the mixed solutions were boiled for 5 min at 100°C. Each boiled sample (15  $\mu$ L) was injected into the stacking gel and the electrophoresis was performed using a Mini-PROTEAN 3 Cell (Bio-Rad

Laboratories, Hercules, CA, USA) under a current of 12 mA. The obtained gels were stained for 45 min in the presence of 0.25% Coomassie Brilliant Blue R-250 solution and then destained with a mixed solvent containing 5% methanol and 7.5% acetic acid until the bands were clear.

### FTIR

All collagen samples were equilibrated in a desiccator for 3 days at 25°C before measurements. Then approximately 3 mg of each collagen sample was homogeneously triturated with 300 mg potassium bromide (KBr) and the mixtures were made into disks under a pressure of 20 MPa. The FTIR spectra were recorded by a Nicolet iS10 spectrometer (Thermo Fisher Scientific, Waltham, MA, USA) at the wavenumbers ranging from 4000 to 500  $\text{cm}^{-1}$  with a resolution of 2  $\text{cm}^{-1}$  at 25°C.

### Thermal Analysis

The thermal stability of collagen was measured by using a VP-DSC microcalorimeter (Microcal, Northampton, USA) over the temperature range of 25-60°C at a constant heating rate of 90°C/h. Collagen solution (0.5 mg/mL) samples and the reference (0.5 M acetic acid) were degassed sufficiently after injecting into the cells. All measurements were performed in triplicate. Based on the VP-DSC data, the plots of molar excess heat capacity  $C_p$  (cal/°C) versus temperature were made.

### Fluorescence Measurements

Fluorescence measurements of collagen solutions containing pyrene were performed at 25°C using a Hitachi F-7000 fluorescence spectrophotometer (Hitachi, Tokyo, Japan) according to the method of Nakashima et al<sup>34</sup> with slight modifications. In brief, pyrene, a hydrophobic probe, was dissolved in methanol to reach a final concentration of 400  $\mu\text{M}$ . Then 50  $\mu\text{L}$  of the stock solution was transferred to a brown glass volumetric flask and mildly evaporated in the presence of nitrogen gas stream. After mixing with collagen solutions, the collagen-pyrene mixed samples were fully homogenized with the aid of ultrasound (120 W) using an ultrasonic equipment (KQ 3200B, Kunshan Instrument, China). Subsequently, the solution samples were stored in darkness at 4°C for 24 h before measurements. The fluorescence spectra for each sample were collected in triplicate by excitation at 343 nm and emission at 360-460 nm. All measurements were performed with a scanning rating of 60 nm/min and the slits for excitation and emission were both fixed at 2.5 nm.

### AFM

Collagen samples (0.5 mg/mL) were diluted to 25  $\mu\text{g/mL}$  with 0.5 M acetic acid by gentle stirring, followed by equilibrating at 4°C overnight. A droplet of each collagen sample (15  $\mu\text{L}$ ) was immediately spread on freshly cleaved mica plates and dried at 25°C for 48 h. The surface morphology of the dried collagen samples was observed in the soft tapping mode by using AFM

(Shimadzu SPM 9600, Kyoto, Japan), which was equipped with a pinpoint (Tap150 AI-G, Budget Sensors, Sofia, Bulgaria). The AFM measurements were performed with a scanning rate of 1 Hz and at least three different spots were checked for each sample to ensure the reproducibility.

## Results and Discussion

### Effect of ILs on Calf Skin

Figure 1 shows the histological analysis images of IPS (Figure 1B~G) pretreated with different ILs parameters, in comparison with NS (Figure 1A) displaying the normal fiber structure of calf skin. Because of the ILs pretreatments, the collagen fibers in IPS tended to be looser and far more sparsely distributed. This could be likely due to the disrupting of intermolecular hydrogen bonds and ionic bonds in collagen tissues, not only by the bulky [EMIM]<sup>+</sup> that have the capability to donate proton, but also by the minor proton-accepting anions including [N(CN)<sub>2</sub>]<sup>-</sup> and [BF<sub>4</sub>]<sup>-</sup>. Note that several imidazolium based ILs such as [EMIM]Cl, [BMIM]Cl, and [BMIM][BF<sub>4</sub>] were reported to exhibit excellent efficacy of fiber opening towards goat skins.<sup>11-13</sup> Compared with the histological appearance of limed bovine splits pretreated by EDTA and HCl reported in Li et al.,<sup>6</sup> much larger spacing among adjacent fiber bundles could be observed in IPS, indicating the great fiber opening efficacy of ILs. As the increase of ILs concentration, the pretreated tissues seem to be much looser (see Figure 1B~D or Figure 1E~G). Moreover, at the same concentration of ILs, BPS (e.g. BPS30, Figure 1E) shows a greater extent of fiber opening than APS (e.g. APS30, Figure 1B), possibly owing to the higher polarity of [EMIM]BF<sub>4</sub> than that of [EMIM]N(CN)<sub>2</sub>. Such differences in fiber opening phenomena might be attributed to the lyotropic action and reorientation of the hydration network of collagen induced by ILs with different polarity.<sup>11,14</sup> SEM was performed to further investigate the fiber morphology of NS and IPS at a higher magnification of 3000×. As shown in Figure 2, the skin tissues after pretreatments by ILs clearly exhibit looser fibers compared to NS. On the whole, the effects of ILs types and concentrations on the morphology of collagen fibers were in good agreement with the aforementioned histological analysis.

### Extraction Rate Analysis

The yields of collagens extracted under different conditions are shown in Figure 3. Due to the more opening fibrous structure induced by ILs pretreatments, the extraction rates of IPC are higher than those of NC by 3.84% ~ 9.42% (see Figure 3). Moreover, as the increase of ILs concentration, the extraction rate of collagen became much higher. For instance, the extraction rates of APC30 and APC70 increased accordingly from 23.21% to 28.79%. Furthermore, the extraction rates of BPC were slightly higher than those of APC, conforming to the dispersion trend of collagen fibers induced by ILs with different polarity. The

opened fibrous structure of ILs pretreated skins should be beneficial for the penetration of acetic acid and pepsin into the skin matrix during collagen extraction, leading to an increased yield of collagen. Therefore, the ILs pretreatment could be applied as an effective and green approach to improve the extraction rate of collagen. Compared with the EDTA

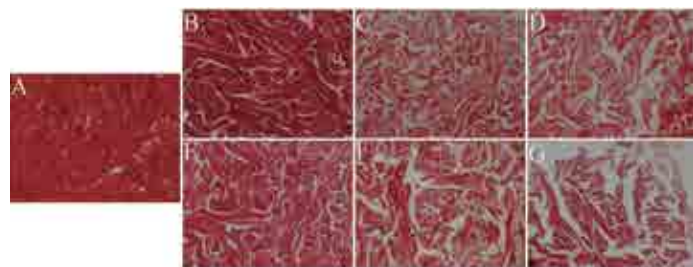


Figure 1. Effect of ionic liquids pretreatment on histological appearance of calf skin. Histological appearances of NS and IPS (APS and BPS) treated by hematoxylin-eosin staining at a magnification of 20×. (A) NS, (B) APS30, (C) APS50, (D) APS70, (E) BPS30, (F) BPS50, and (G) BPS70.

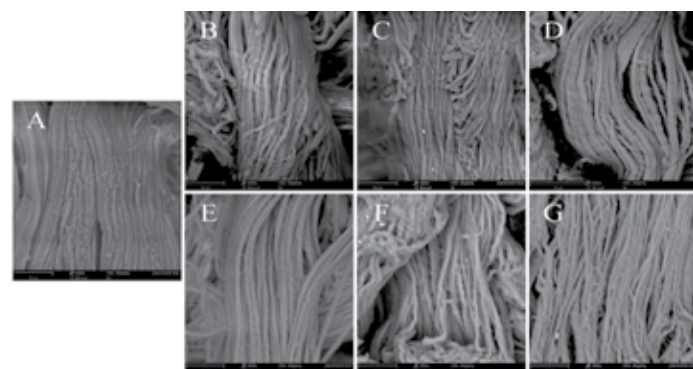


Figure 2. SEM images of NS and IPS (APS and BPS) at a magnification of 3000×. (A) NS, (B) APS30, (C) APS50, (D) APS70, (E) BPS30, (F) BPS50, and (G) BPS70.

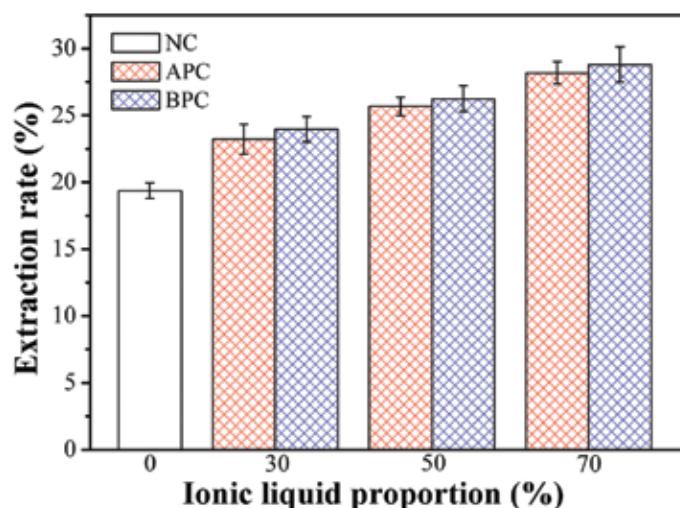


Figure 3. Extraction rates of IPC (APC and BPC) at different ionic liquid proportions, in comparison with that of NC.

pretreatment of limed bovine splits reported by Li et al.,<sup>6</sup> in which the collagen yield was increased from 4.17% (without pretreatment) to 10.42% (after pretreatment) with an increment of 6.25%, the increase of collagen yields induced by ILs pretreatments of calf skins could reach up to 9.42%, indicating the high efficiency of ILs pretreatments for collagen extraction.

### Structural Integrity of Collagen

The ILs pretreatments of calf skins should be premised on the preservation of the triple helix structure of collagen. Firstly, SDS-PAGE was performed to check the subunit composition of IPC, along with NC as a comparison. As shown in Figure 4, all collagen samples are composed of two distinct  $\alpha$  chains ( $\alpha 1$  and  $\alpha 2$ ) and one  $\beta$  chain (dimers of  $\alpha$  chains) as the major constituents. These SDS-PAGE patterns agreed with those of type I collagen from limed bovine splits as previously reported,<sup>6,31</sup> indicating a molecular mass of 300 kDa similar to that of native collagen molecules. Furthermore, it should be emphasized that the appearance of electrophoretic bands lower than 100 kDa is an unambiguous indication of the damage of collagen structure.<sup>8</sup> However, such small components were not detected in this study, suggesting that no degradation of collagen polypeptide chains occurred during the ILs pretreatments. Thus, the SDS-PAGE results confirmed the structural integrity and high purity of calf skin collagen.

In addition, to further verify the triple helix conformation of collagen, the secondary structure of NC and IPC was examined by using FTIR. As shown in Figure 5, all collagen samples exhibit the presence of five characteristic FTIR peaks including amide A, B, I, II, and III, which are typical for type I collagen.<sup>7</sup> The amide A bands of  $3400\text{ cm}^{-1}$  are related to the hydrogen-bonded -NH groups, while the amide B bands reflecting C-H stretching are found at  $2940\text{ cm}^{-1}$ .<sup>35</sup> The amide I bands at  $1650\text{ cm}^{-1}$  are attributed to C=O stretching vibrations in the polypeptide backbone, and the amide II bands at  $1550\text{ cm}^{-1}$  are initiated from N-H bending and C-H stretching. The bands at  $1245\text{ cm}^{-1}$  representing amide III are dominated by the C-H vibrations.<sup>36</sup> On the whole, although the FTIR spectra for different collagens seemed to be similar, there were some differences in the peak location and intensity, indicating that the ILs pretreatments might induce slight changes in the secondary structure of collagen. Nevertheless, the absorption ratios between the amide III and  $1454\text{ cm}^{-1}$  bands for all collagens were nearly 1.0, unambiguously suggesting that the triple-helical structure of collagen was preserved.<sup>8,37</sup> Overall, the FTIR analysis supported the structural integrity of collagen, conforming to the above SDS-PAGE results.

### Thermal Stability of Collagen

Figure 6(a) shows the temperature dependence of the specific heat capacity ( $C_p$ ) of different calf skin collagens. Except for BPC70, all other collagen samples displayed two endothermic

peaks, respectively. The first minor peaks at relatively lower temperatures were originated from the breaking of hydrogen bonds among collagen aggregates, while the major peaks at higher temperatures were attributed to the helix-coil transition of collagen molecules.<sup>4,5</sup> Thus, in this work, the values of the major peaks ( $T_m$ ) and the corresponding enthalpy changes ( $\Delta H$ ) were used to evaluate the thermal stability of collagen, as shown in Table I. The higher the values of  $T_m$  and  $\Delta H$ , the better the thermal stability of collagen. According to Table I, the  $T_m$  and  $\Delta H$  values of IPC are slightly lower than those of NC, respectively. Moreover, the values of  $T_m$  and  $\Delta H$  showed a tiny downward trend with the increase of ILs concentration and polarity, possibly due to the different extent of rupturing of hydrogen bonds during ILs pretreatments. It should be recognized that the

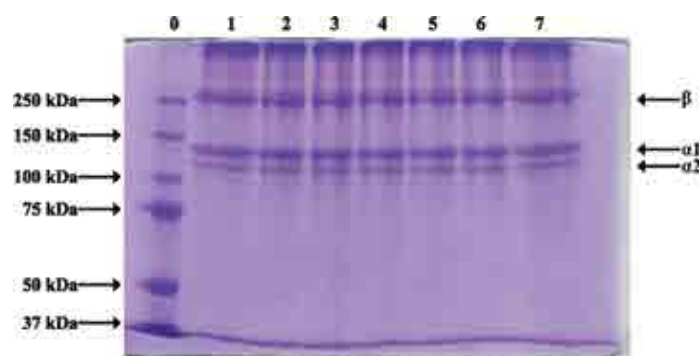


Figure 4. SDS-PAGE patterns of NC and IPC (APC and BPC). Lane 0: protein molecular weight marker; lanes 1-7: NC, APC30, APC50, APC70, BPC30, BPC50, and BPC70, respectively.

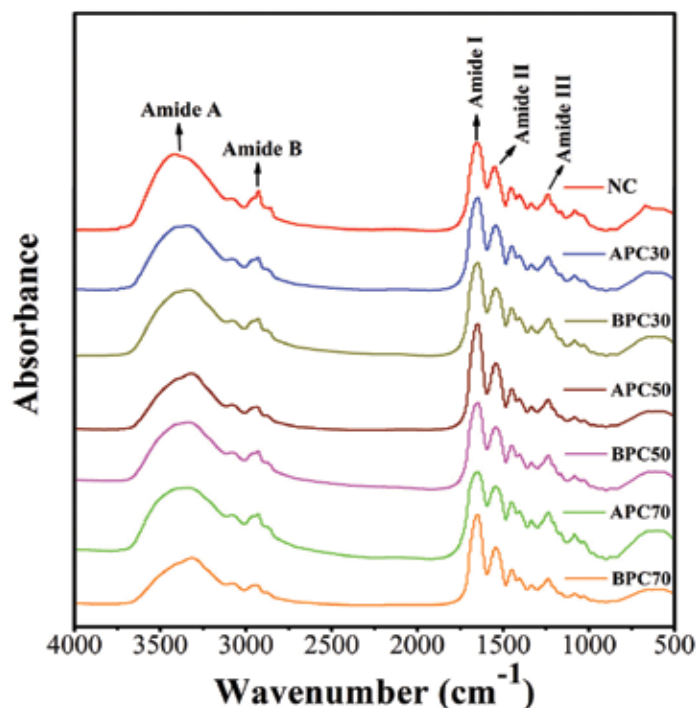


Figure 5. FTIR spectra of NC and IPC (APC and BPC).

disappearance of a minor peak for BPC70 compared with other IPC might have a close relation to the strong polarity of [EMIM][BF<sub>4</sub>] at the concentrations of 70% (w/w) during pretreatment.

It has been well-known that intra-molecular hydrogen bonding plays an essential role in stabilizing the triple-helix structure of collagen.<sup>1,4,5</sup> During the ILs pretreatment of calf skins, most ruptured hydrogen bonds should be of inter-molecular nature, while the intra-molecular hydrogen bonds were only partially disrupted, as indicated by the slight decrease of  $T_m$  (<1°C) from NC to BPC70. Note that it is the serious destruction of collagen structure that is always accompanied with a significant decrease in its thermal denaturation temperature.<sup>9,15,20</sup> Therefore, the intra-molecular triple helix structure of calf skin collagens extracted in this work remains intact, which was also supported by the aforementioned SDS-PAGE and FTIR analyses.

#### Aggregation Behavior of Collagen

The thermal stability of collagen is closely correlated to its aggregation state in solution,<sup>4</sup> so pyrene fluorescence analysis was performed to explore the aggregation behavior of calf skin collagens. Pyrene, a sensitive hydrophobic fluorescence probe, is widely adopted to determine the alterations in polarity of its surrounding micro-environment.<sup>38</sup> Pyrene can incorporate into the hydrophobic cores formed by the self-aggregation of collagen molecules in solution, resulting in the changes of fluorescence intensity.<sup>39</sup> Figure 6(b) displays the pyrene fluorescence emission spectra of different calf skin collagens. As shown in Figure 6(b), all collagen samples indicate four characteristic emission peaks at ~374, ~379, ~384, and ~394 nm, respectively, agreeing well

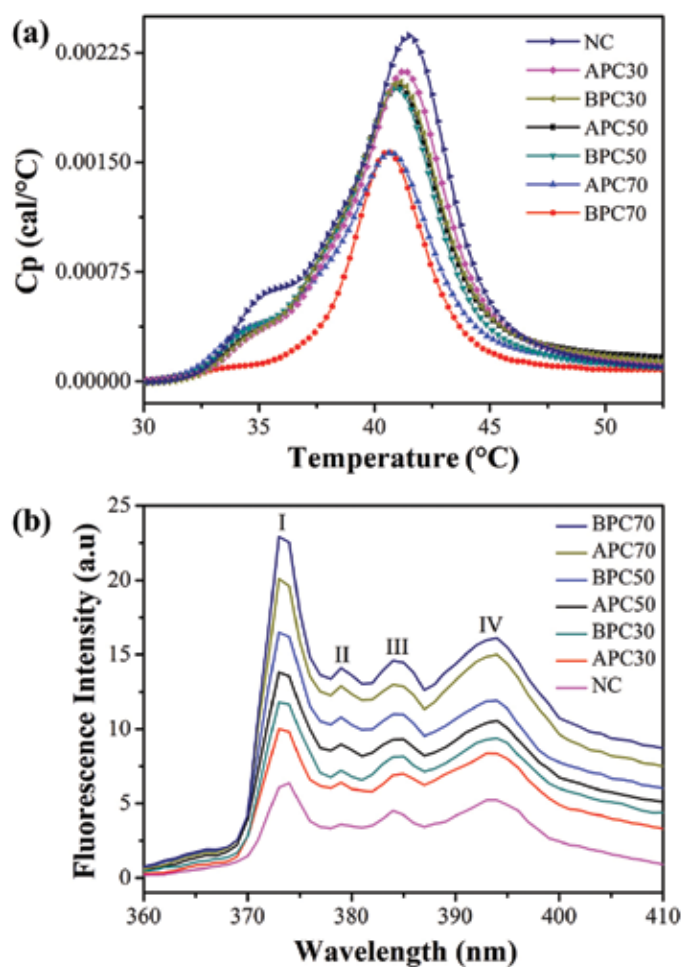


Figure 6. The (a) thermal transition curves and (b) pyrene fluorescence emission spectra of NC and IPC (APC and BPC).

**Table I**  
Values of VP-DSC thermodynamic parameters ( $T_m$  and  $\Delta H$ ) and pyrene fluorescence intensity ratio ( $I_1/I_3$ ) for different collagen solutions.

Collagen Sample	Thermodynamic parameters		Fluorescence intensity ratio
	$T_m$ (°C)	$\Delta H$ (kJ/mol)	$I_1/I_3$
NC	41.495 ± 0.053	0.0161 ± 0.0026	1.389 ± 0.014
APC30	41.286 ± 0.026	0.0158 ± 0.0014	1.431 ± 0.008
BPC30	41.124 ± 0.012	0.0142 ± 0.0009	1.445 ± 0.011
APC50	40.903 ± 0.041	0.0140 ± 0.0024	1.480 ± 0.005
BPC50	40.831 ± 0.034	0.0133 ± 0.0035	1.501 ± 0.009
APC70	40.615 ± 0.022	0.0109 ± 0.0011	1.547 ± 0.012
BPC70	40.503 ± 0.017	0.0084 ± 0.0017	1.570 ± 0.007

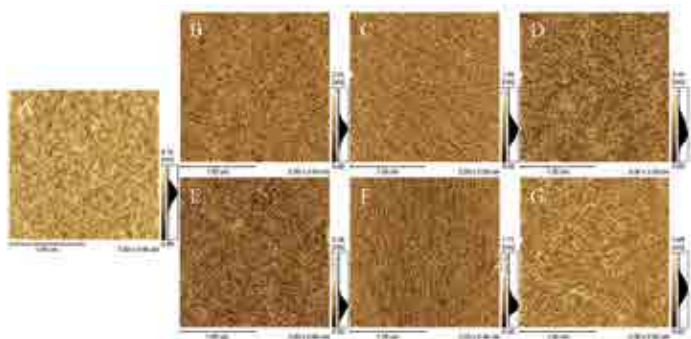


Figure 7. AFM images of NC and IPC (APC and BPC). (A) NC, (B) APC30, (C) APC50, (D) APC70, (E) BPC30, (F) BPC50, and (G) BPC70.

with previous investigations.<sup>40</sup> Furthermore, it is well-known that the fluorescence intensity ratio of the first to the third peak ( $I_1/I_3$ ) can be used to detect the polarity of the micro-environment surrounding the probe.<sup>4</sup> Such a ratio is relatively higher and lower in a polar and hydrophobic environment, respectively. As demonstrated in Table I, the  $I_1/I_3$  values of IPC are slightly higher than that of NC, and tend to increase as increasing ILs concentration and polarity, suggesting the significant impacts of ILs pretreatments on the aggregation state of collagen. One explanation might be that the inter-molecular hydrogen bonds of collagen were ruptured to different extents by ILs pretreatments. For NC with no ILs pretreatment, the extracted collagen molecules were easier to self-aggregate and form hydrophobic cores due to the unruptured inter-molecular hydrogen bonds, resulting in a more hydrophobic micro-environment for pyrene and the lower  $I_1/I_3$  value. In contrast, for IPC subjected to the ILs pretreatments, the polarity of pyrene micro-environment was enhanced and the  $I_1/I_3$  values became higher. Overall, the higher the ILs concentration and polarity, the higher the  $I_1/I_3$  values and the weaker the collagen aggregation.

AFM was used to further determine the changes in aggregation state and morphology of NC and IPC. As shown in Figure 7A, NC exhibits a characteristic entangled collagen fibrous network due to the inherent self-aggregation of collagen molecules. Moreover, owing to the ILs pretreatments, the collagen fibers in IPC (Figure 7B~G) display an obvious tendency of sparse distribution, particularly with the increase of ILs concentration and polarity. In whole, the weaker aggregated state of IPC was consistent with the above pyrene fluorescence analysis.

## Conclusions

The fiber contexture of calf skins and the structure and properties of the extracted collagens were highly dependent on the ILs species and concentration. ILs pretreatments could loosen the skin fibers and thereby improved the extraction rate

of collagen. The triple helix structural integrity of collagen was maintained, although there was a slight decrease in its thermal stability. The collagen aggregation became weaker as the increase of ILs concentration and polarity. The ILs pretreatments are expected to be used as a greener approach for collagen extraction and are beneficial for preparing high yield and quality collagen for biomedical applications.

## Acknowledgements

The authors gratefully acknowledge the financial supports from the National Natural Science Foundation of China (Nos. 21776184 and 21606156). The authors would thank Zhonghui Wang (College of Biomass Science and Engineering, Sichuan University) for her help in VP-DSC and AFM observations.

## References

- Shoulders, M. D., and Raines, R. T.; Collagen structure and stability, *Annu. Rev. Biochem.* **78**, 929-958, 2009.
- Lin, K., Zhang, D., Macedo, M. H., Cui, W., Sarmento, B., and Shen, G.; Advanced Collagen-Based Biomaterials for Regenerative Biomedicine, *Adv. Funct. Mater.* **29**, 1804943, 2019.
- Liu, W., Li, G., Miao, Y., and Wu, X.; Preparation and characterization of pepsin solubilized type I collagen from the scales of snakehead (*Ophiocephalus argus*). *J. Food Biochem.* **33**, 20-37, 2009.
- Yang, H., Li, Q., Liu, S., and Li, G.; Acetic acid/1-ethyl-3-methylimidazolium acetate as a biphasic solvent system for altering the aggregation behavior of collagen molecules. *J. Mol. Liq.* **262**, 78-85, 2018.
- Liu, W., and Li, G.; Non-isothermal kinetic analysis of the thermal denaturation of type I collagen in solution using isoconversional and multivariate non-linear regression methods. *Polym. Degrad. Stabil.* **95**, 2233-2240, 2010.
- Li, D., Yang, W., and Li, G. Y.; Extraction of native collagen from limed bovine split wastes through improved pretreatment methods. *J. Chem. Technol. Biotechnol.* **83**, 1041-1048, 2008.
- Xu, S., Yang, H., Shen, L., and Li, G.; Purity and yield of collagen extracted from Southern catfish (*Silurus meridionalis* Chen) skin through improved pretreatment methods. *Int. J. Food Prop.* **20**, s141-s153, 2017.
- Liu, W., Zhang, Y., Cui, N., and Wang, T.; Extraction and characterization of pepsin-solubilized collagen from snakehead (*Channa argus*) skin: Effects of hydrogen peroxide pretreatments and pepsin hydrolysis strategies. *Process Biochem.* **76**, 194-202, 2019.

9. Hu, Y., Liu, L., Dan, W., Dan, N., and Gu, Z.; Evaluation of 1-ethyl-3-methylimidazolium acetate based ionic liquid systems as a suitable solvent for collagen. *J. Appl. Polym. Sci.* **130**, 2245-2256, 2013.
10. Liu, J., Xu, Z., Chen, Y., Fan, H., and Shi, B.; 1-butyl-3-methylimidazolium acetate as an alternative solvent for type I collagen. *JALCA* **109**, 189-196, 2014.
11. Mehta, A., Rao, J. R., and Fathima, N. N.; Effect of ionic liquids on the different hierarchical order of type I collagen. *Colloid Surf. B-Biointerfaces* **117**, 376-382, 2014.
12. Alla, J. P., Rao, J. R., and Fathima, N. N.; Integrated depilation and fiber opening using aqueous solution of ionic liquid for leather processing. *ACS Sustain. Chem. Eng.* **5**, 8610-8618, 2017.
13. Jayakumar, G. C., Mehta, A., Rao, J. R., and Fathima, N. N.; Ionic liquids: new age materials for eco-friendly leather processing. *RSC Adv.* **5**, 31998-32005, 2015.
14. Harada, L. K., Pereira, J. F. B., Campos, W. F., Silva, E. C., Moutinho, C. G., Vila, M. M. D. C., Oliveira Jr., J. M., Teixeira, J. A., Balcão, V. M., and Tubino, M.; Insights into Protein-Ionic Liquid Interactions Aiming at Macromolecule Delivery Systems. *J. Braz. Chem. Soc.* **29**, 1983-1998, 2018.
15. Meng, Z., Zheng, X., Tang, K., Liu, J., Ma, Z., and Zhao, Q.; Dissolution and regeneration of collagen fibers using ionic liquid. *Int. J. Biol. Macromol.* **51**, 440-448, 2012.
16. Pei, Y., Chu, S., Zheng, Y., Zhang, J., Liu, H., Zheng, X., and Tang, K.; Dissolution of Collagen Fibers from Tannery Solid Wastes in 1-Allyl-3-methylimidazolium Chloride and Modulation of Regenerative Morphology. *ACS Sustain. Chem. Eng.* **7**, 2530-2537, 2019.
17. Li, Q., Xu, B., Xu, X., Zhuang, L., Wang, Q., and Wang, G.; Dissolution and interaction of white hide powder in [Etmim][C<sub>12</sub>H<sub>25</sub>SO<sub>4</sub>]. *J. Mol. Liq.* **241** 974-983, 2017.
18. Li, Q., Xu, B., Yan, W., Zhuang, L., Qiang, W., Chao, L., Xu, X., and Wang, G.; Effect of cationic structure of ionic liquids on dissolution and regeneration of white hide powder. *Fiber. Polym.* **18**, 1512-1522, 2017.
19. Wang, G., Guo, J., Zhuang, L., Wang, Y., and Xu, B.; Dissolution and regeneration of hide powder/cellulose composite in Gemini imidazolium ionic liquid. *Int. J. Biol. Macromol.* **76**, 70-79, 2015.
20. Muhammad, N., Gonfa, G., Rahim, A., Ahmad, P., Iqbal, F., Sharif, F., Khan, A. S., Khan, F. U., Khan, Z. U. L. H., Rehman, F., and Rehman, I. U.; Investigation of ionic liquids as a pretreatment solvent for extraction of collagen biopolymer from waste fish scales using COSMO-RS and experiment. *J. Mol. Liq.* **232**, 258-264, 2017.
21. Tarannum, A., Muvva, C., Mehta, A., Rao, J. R., and Fathima, N. N.; Phosphonium based ionic liquids-stabilizing or destabilizing agents for collagen? *RSC Adv.* **6**, 4022-4033, 2016.
22. Tarannum, A., Jonnalagadda, R. R., and Nishter, N. F.; Stability of collagen in ionic liquids: Ion specific Hofmeister series effect. *Spectrosc. Acta Pt. A-Molec. Biomolec. Spectrosc.* **212**, 343-348, 2019.
23. Reddy, R. R., Ganesh, S., Balaraman, M., and Kumar, B. V. N. P.; Selective binding and dynamics of imidazole alkyl sulfate ionic liquids with human serum albumin and collagen - a detailed NMR investigation. *Phys. Chem. Chem. Phys.* **20**, 9256-9268, 2018.
24. Tarannum, A., Adams, A., and Fathima, N. N.; Impact of Ionic Liquids on the Structure and Dynamics of Collagen. *J. Phys. Chem. B* **122**, 1060-1065, 2018.
25. Tarannum, A., Rao, J. R., and Fathima, N. N.; Choline Based Amino Acid ILs-Collagen Interaction: Enunciating its Role in Stabilization/destabilization Phenomena. *J. Phys. Chem. B* **122**, 1145-1151, 2018.
26. Tarannum, A., Muvva, C., Mehta, A., Rao, J. R., and Fathima, N. N.; Role of Preferential Ions of Ammonium Ionic Liquid in Destabilization of Collagen. *J. Phys. Chem. B* **120**, 6515-6524, 2016.
27. Carvalho, R. N. L., Lourenço, N. M. T., Gomes, P. M. V., and Fonseca, L. J. P.; Swelling behavior of gelatin-ionic liquid functional polymers. *J. Polym. Sci., Part B: Polym. Phys.* **51**, 817-825, 2013.
28. Earle, M. J., and Seddon, K. R.; Ionic liquids. Green solvents for the future. *Pure Appl. Chem.* **72**, 1391-1398, 2000.
29. Swatloski, R. P., Spear, S. K., Holbrey, J. D., and Rogers, R. D.; Dissolution of Cellulose with Ionic Liquids. *J. Am. Chem. Soc.* **124**, 4974-4975, 2002.
30. Xie, H., Zhang, S., and Li, S.; Chitin and chitosan dissolved in ionic liquids as reversible sorbents of CO<sub>2</sub>. *Green Chem.* **8**, 630-633, 2006.
31. Zhang, Z. K., Li, G. Y., and Shi, B. L.; Physicochemical properties of collagen, gelatin and collagen hydrolysate derived from bovine lamed split wastes. *J. Soc. Leather Technol. Chem.* **90**, 23-28, 2006.
32. Yunoki, S., Nagai, N., Suzuki, T., and Munekata, M.; Novel biomaterial from reinforced salmon collagen gel prepared by fibril formation and cross-linking. *J. Biosci. Bioeng.* **98**, 40-47, 2004.
33. Laemmli, U. K.; Cleavage of Structural Proteins during the Assembly of the Head of Bacteriophage T4. *Nature* **227**, 680-685, 1970.
34. Nakashima, K., Anzai, T., and Fujimoto, Y.; Fluorescence Studies on the Properties of a Pluronic F68 Micelle. *Langmuir* **10**, 658-661, 1994.
35. Yan, M., Li, B., Zhao, X., and Ren, G.; Characterization of acid-soluble collagen from the skin of walleye pollock (Theragra chalcogramma). *Food Chem.* **107**, 1581-1586, 2008.

36. Li, Z.R., Wang, B., Chi, C.F., and Zhang, Q.H.; Isolation and characterization of acid soluble collagens and pepsin soluble collagens from the skin and bone of Spanish mackerel (*Scomberomorus niphonius*). *Food Hydrocolloid*. **31**, 103–113, 2013.
  37. Liu, D., Wei, G., Li, T., Hu, J., Lu, N., Regenstein, J. M., and Zhou, P.; Effects of alkaline pretreatments and acid extraction conditions on the acid-soluble collagen from grass carp (*Ctenopharyngodon idella*) skin. *Food Chem*. **172**, 836-843, 2015.
  38. Hamley, I. W., Dehsorkhi, A., Castelletto, V., Walter, M. N. M., Connon, C. J., Reza, M., and Ruokolainen, J.; Self-Assembly and Collagen-Stimulating Activity of a Peptide Amphiphile Incorporating a Peptide Sequence from Lumican. *Langmuir* **31**, 4490-4495, 2015.
  39. Guan, J.-Q., and Tung, C.-H.; Aggregation of Novel Betaine Surfactants N-(3-Alkoxy-2-hydroxypropyl)-N,N-dimethylglycines in Aqueous Solution: Micellization and Microenvironment Characteristics. *Langmuir* **15**, 1011-1016, 1999.
  40. Basu Ray, G., Chakraborty, I., and Moulik, S. P.; Pyrene absorption can be a convenient method for probing critical micellar concentration (cmc) and indexing micellar polarity. *J. Colloid Interface Sci*. **294**, 248-254, 2006.
-